

Structure of different grades of nuclear graphite

This article has been downloaded from IOPscience. Please scroll down to see the full text article.

2012 J. Phys.: Conf. Ser. 371 012017

(<http://iopscience.iop.org/1742-6596/371/1/012017>)

View [the table of contents for this issue](#), or go to the [journal homepage](#) for more

Download details:

IP Address: 130.88.107.192

The article was downloaded on 12/10/2012 at 14:09

Please note that [terms and conditions apply](#).

Structure of different grades of nuclear graphite

B E Mironov^{1*}, A V K Westwood¹, A J Scott¹, R Brydson¹, A N Jones²

¹Institute for Materials Research, University of Leeds, Leeds, LS2 9JT, UK

²Nuclear Graphite Research Group, Materials Performance Centre, University of Manchester, Manchester, M60 1QD, UK

*E-mail: pmbem@leeds.ac.uk

Abstract. Owing to its low neutron absorption cross-section, large scattering cross section and thermal and chemical stability, graphite is a key component of operational nuclear reactors where it is used as a moderator, reflector and as major structural component for 90% of current UK nuclear plants. It is also of interest for use in developing the future high temperature gas-cooled reactors. The properties of the nuclear graphite are influenced by its structural characteristics, which change as a function of neutron irradiation, temperature and oxidation. The principal structural changes during neutron irradiation that affect the integrity and dimensions of nuclear graphite components, thereby affecting service lifetime, are that the a-axis contracts and the c-axis expands in the crystallites. Characterization of virgin graphite structure and of the damage evolution after irradiation of nuclear graphite has an important role to play in the understanding and development of materials used in current and future nuclear reactors, respectively.

1. Introduction

Graphite is a key component of operational nuclear reactors where it is used as a moderator, reflector and for other structural components in 90% of current UK nuclear plants and is proposed for use in future high temperature gas-cooled reactors.

Inside a reactor, fast neutron irradiation significantly changes the crystallite size and influences bulk property changes. The solidity and working life of reactor components is influenced by dimensional change, by creep and weight loss, amongst other properties [1]. These effects however are not completely understood and the body of current data regarding irradiation of nuclear graphite is incomplete.

Graphite is used as a moderator due to its low absorption cross section and high scattering cross section compared to other materials. Neutron impact leads to carbon atom displacements which damage the graphite lattice and change the crystallite size and spacing [1,2]. Characterization of the virgin nuclear graphite structure and of the evolution of damage after irradiation has an important role to play in developing a comprehensive understanding of the working behaviour of current nuclear graphite. This will also have a major role in the development of material for use in future nuclear reactors.

This work aims to characterise two types of graphite in terms of differing crystallinity using techniques such as Raman spectroscopy, X-ray diffraction (XRD) and electron microscopy. The graphite employed are from two Gen I and Gen II UK nuclear plants materials, namely; “Pile Grade A” (PGA) and “Gilsocarbon” (GIL). Both of these materials are based on a filler and a binder, petroleum coke and asphalt coke as a filler in PGA and GIL respectively, mixed and formed with pitch binder, then baked and finally graphitised at high temperature ($\sim 3000^\circ\text{C}$).

2. Experimental

The samples of PGA and GIL were machined with a Struers Accutome-2 cutting machine at a speed of 1200rpm/sec for Raman spectroscopy, XRD and Scanning Electron Microscopy (SEM) analyses, while for Transmission Electron Microscopy (TEM), samples were either ground, dispersed in acetone and drop cast onto a carbon grid or using Focused Ion Beam (FIB) sections made in an FEI Nova200.

For SEM studies an FEI XL30 was used operating at 3keV while TEM analysis was conducted on an FEI Tecnai F20 FEG-TEM operating at 200kV and equipped with a CCD camera. Raman spectra were collected from 1cm thick sample slices using a commercial Renishaw Invia micro-Raman spectrometer equipped with a CCD detector and a modified optical microscope. The spectra were recorded for 10 sec/acquisition with a number of 10 acquisitions/sample. We used a 514.5nm Ar/Kr ion laser with $P=25\text{mW}$ and a 50X objective lens for focusing the laser light onto the samples. X-ray diffraction patterns were recorded on a Philips X'Pert diffractometer, making use of a copper X-ray source ($\lambda_{\text{K}\alpha 1} = 0.15405\text{ nm}$) and working in θ - 2θ mode with X'pertCollector software.

3. Results and discussion

The characterization of the two nuclear graphites that we studied (PGA and GIL) began with the morphology characterization. It was observed by SEM, that the porosity is very high ($\sim 20\%$ after impregnation with pitch and 25% before that) [1], with GIL having a slightly lower porosity (with a density $\sim 1.81\text{g/cm}^3$) compared with PGA (density $\sim 1.74\text{g/cm}^3$). Also the coke particles look different in shape and size with PGA showing needle shaped filler particles relative to GIL (Fig.1), this aspect is due to differences in manufacturing procedure and materials used. The differences between PGA and GIL are that PGA has anisotropic properties as it is made using extrusion which imparts preferred orientation to the coke particles, while GIL is semi-isotropic, made by moulding of particles which have an “onion” like structure with random orientation

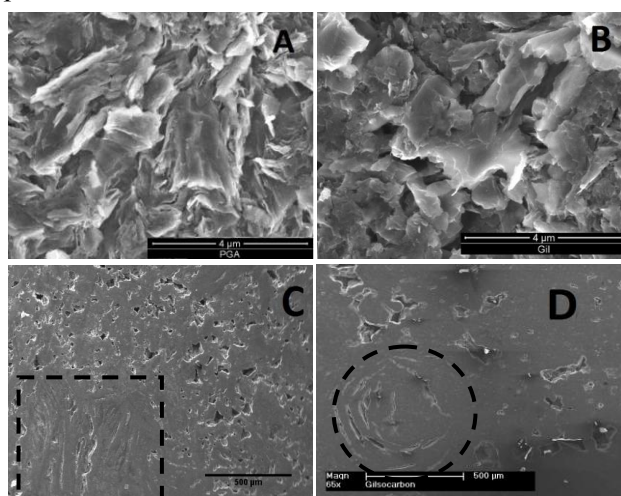


Figure 1. SE image taken in SEM of: typical needle like platelets of PGA(A) and GIL(B) in random orientation; Surface of PGA(C) and GIL(D) - dotted lines denote the filler particles specific porosity, longitudinal cracks for PGA and circular cracks for GIL

The pores observed were distinctive for both the filler and binder. For the filler part of the graphite, highlighted with dotted circles (Fig.1 C-D), elongated pores follow the structure of the filler particles, needle-shape particles for PGA (Fig.1 C) and onion like-circular structures for GIL (Fig.1 D).

Raman analysis of both graphites was used in order to determinate the disorder present inside the structure. Two peaks could be observed that are characteristic of (nuclear) graphite [4]: the D peak (disorder $\sim 1354\text{cm}^{-1}$) and the G peak (order $\sim 1583\text{cm}^{-1}$). A second order feature could also be detected ($\sim 2708\text{cm}^{-1}$) for both samples. The ratio of the intensities of these peaks, I_D/I_G , was lower for PGA than for GIL (Fig.2) reflecting a larger crystallite size which can be attributed to a textured product. From this ratio it is also

possible to calculate the value for the coherence length in the **a**-direction, L_a , using a corrected version of Tuinstra-Koenig [5] formula:

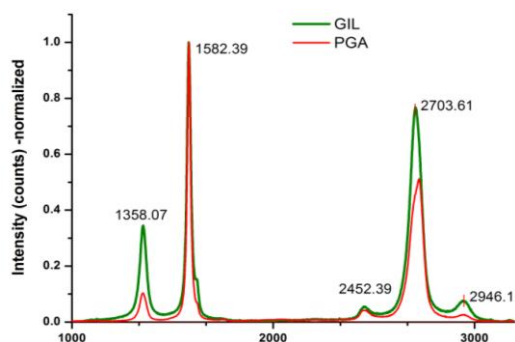


Figure 2. Raman spectra of PGA and GIL

$$L_a(\text{nm}) = C(\lambda) \left(\frac{I_D}{I_G} \right)^{-1}, \text{ where } C(514.5\text{nm}) \sim 4.4.$$

The calculated values of L_a for PGA and GIL were $21 \pm 4\text{nm}$ and $20 \pm 1\text{nm}$, respectively. The difference in standard deviation values may be due to variation in coherence lengths within the samples (presence of filler or binder in the acquiring spot) coupled with the local rather than global nature of this analysis.

XRD was used in order to confirm the Raman results and also to obtain global information regarding crystallite size (coherence length) in the **c**- and **a**-directions [6]. The coherence lengths in the **a** direction were 44.8nm for PGA and 47.2nm for GIL, whereas in the **c** direction the calculated values were 23.7nm for PGA and 35.6nm for GIL. These were calculated using Scherrer's equation ($L = K\lambda/\beta\cos\theta$), where the K constants used were: $K_a = 1.84$ (for **a** direction) and $K_c = 0.9$ (for **c** direction); β represents broadening at half the maximum intensity in radians and θ the angle that corresponds to the measured peak.

Though the L_a values obtained from XRD and Raman have the same order of magnitude, there are clear differences between the values derived from the two techniques. The smaller values obtained from the Raman measurement could be due to the fact that the sample was cut and hence a bigger disorder was created which increased the intensity of the D peak and influenced the calculated Raman values for L_a . We have used Bright Field (BF) TEM to confirm these values.

TEM of the FIB samples of both PGA and GIL gave information about the internal structure of the materials, and showed curved crystallites surrounding voids (Fig.3) which make measurement of the coherence lengths uncertain. For simplicity we report here measurements taken on the crushed and ground materials shown in Fig. 4.

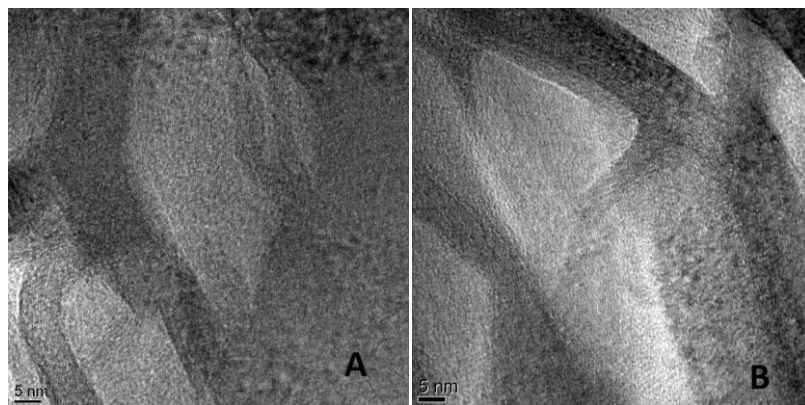


Figure 3. BF TEM images of FIB samples of PGA(A) and GIL (B) in random orientation

The coherence lengths in the **c** direction (L_c) exhibited a large range: between $2\text{-}26\text{nm}$ for PGA and $2\text{-}36\text{nm}$ for GIL. The average of the dimensions of L_c measured from TEM (for PGA $10.3 \pm 7.4\text{nm}$ and for GIL $11.2 \pm 9.1\text{nm}$) were slightly lower than the values from XRD but they showed the same trend with the value for PGA being larger and showing a larger standard deviation than that for GIL.

A histogram of the crystallite size data (L_a) from TEM is shown in Figure 5. Similar to the coherence length in the **c** direction, the two graphites show a large range in L_a . PGA exhibits a range of L_a values for the crystallites between $5\text{-}80\text{nm}$ and for GIL the range was bigger and lay between $5\text{-}200\text{nm}$ or higher. This could explain the discrepancy between Raman, a more local analysing technique, and XRD, a more global analysing technique giving an average value.

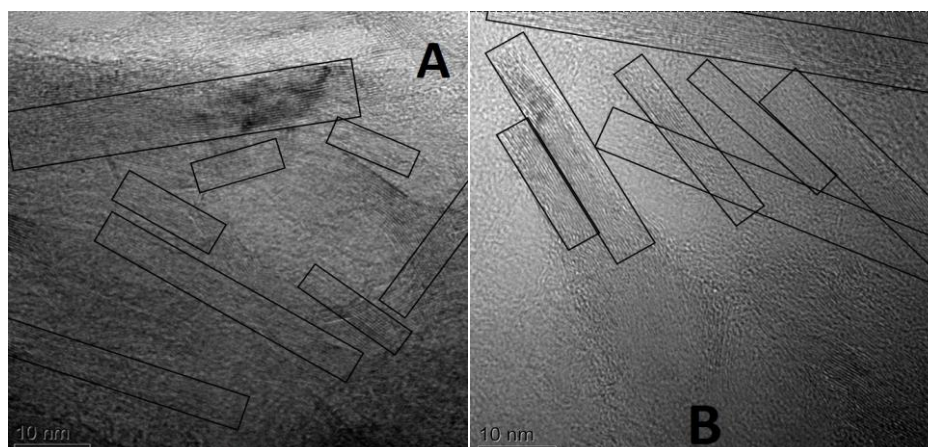


Figure 4. BF TEM images of: powder PGA(A) and GIL (B) with highlighted different size crystallites for both of graphites

From the histogram (Fig.5) of the L_a dimensions measured by TEM, average L_a values of 48 ± 20 nm and 53 ± 38 nm can be calculated for PGA and GIL, respectively. These are close to the ones calculated from the XRD.

As expected from the comparison between XRD and Raman, the L_a values calculated from Raman (PGA $L_a = 21 \pm 4$ nm and GIL $L_a = 20 \pm 11$ nm) were different compared with the ones found by TEM, which could mean that the Raman analysis can only give information regarding the degree of order/disorder in the sample and does not allow precise evaluation of L_a as has been suggested.

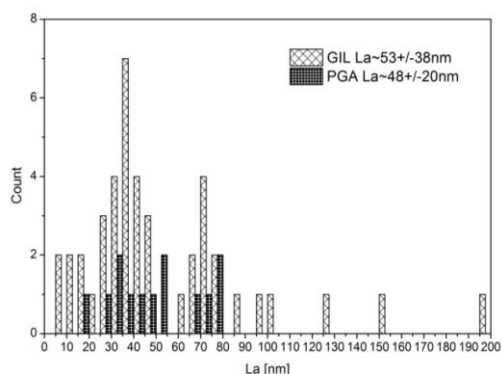


Figure 5. Histogram of dimensions occurrence in both PGA and GIL

4. Conclusions

XRD and Raman investigations of graphite for nuclear applications can provide both global and local information respectively with regards to the order, disorder or crystallite orientation size and spacing. However it is desirable to support these studies with SEM and TEM to understand the details of the microstructure and to minimize ambiguities.

Further investigations of how the structure changes in graphite are influencing the working life of nuclear reactors are needed. Parameters like irradiation duration, dose, gas environment and temperature will be taken in consideration in predicting the failures and operating time of nuclear reactors for further development.

Acknowledgments

The authors would like to acknowledge the financial support of EPSRC (EP/I003312/1) for this project entitled “Fundamentals of current and future uses of Nuclear Graphite”.

References

- [1] Nightingale R 1962 *Nuclear Graphite* Academic Press 87-117
- [2] Simmons JHW 1965 *Radiation Damage in Graphite*
- [3] Thomsen C and Reich R 2004 *Phil. Trans. R. Soc. Lond.* **362** 2271-2288
- [4] Wang Y et.al 1990 *Chem. Mater* **2**, 557-563
- [5] Ferrari AC and Robertson J 2000 *J. Physics Review B* **61** 14095-14107
- [6] Seehra MS and Pavlovic AS 1993 *Carbon* **31** 557-564